Article

Not peer-reviewed version

Defining an Optimal Time Window for Salvage Surgery: Primary Radiochemotherapy Does Not Induce Radiomically Assessable Short-Term Alterations of Skeletal Muscle Composition in Head and Neck Squamous Cell Carcinoma

Matthias Santer , Herbert Riechelmann , Benedikt Hofauer , Joachim Schmutzhard , Wolfgang Freysinger , Annette Runge , Timo Gottfried , Philipp Zelger , Gerlig Widmann , Hanna Kranebitter , Stephanie Mangesius , Julian Mangesius , Florian Kocher , Daniel Dejaco *

Posted Date: 4 September 2023

doi: 10.20944/preprints202309.0068.v1

Keywords: head and neck neoplasms; head and neck cancer; head and neck squamous cell carcinoma; radiotherapy; radiochemotherapy; salvage surgery; time interval; body composition; skeletal muscle; computed tomography scan; radiomics

Article

Defining an Optimal Time Window for Salvage Surgery: Primary Radiochemotherapy Does Not Induce Radiomically Assessable Short-Term Alterations of Skeletal Muscle Composition in Head and Neck Squamous Cell Carcinoma

Matthias Santer [1], Herbert Riechelmann [1], Benedikt Hofauer [1], Joachim Schmutzhard [1], Wolfgang Freysinger [1], Annette Runge [1], Timo Maria Gottfried [1], Philipp Zelger [2], Gerlig Widmann [3], Hanna Kranebitter [3], Stephanie Mangesius [4], Julian Mangesius [5], Florian Kocher [6] and Daniel Dejaco [1,*]

1 Department of Otorhinolaryngology-Head and Neck Surgery, Medical University of Innsbruck, 6020 Innsbruck, Austria; matthias.santer@i-med.ac.at (M.S.); *daniel.dejaco@i-med.ac.at (D.D.); herbert.riechelmann@i-med.ac.at (H.R.); benedikt-gabriel.hofauer@i-med.ac.at (B.H.); joachim.schmutzhard@i-med.ac.at (J.S.); wolfgang.freysinger@i-med.ac.at (W.F.); annette.runge@tirol-kliniken.at (A.R.); timo.gottfried@i-med.ac.at (T.M.G.).

2 Department for Hearing, Voice and Speech Disorders, Medical University of Innsbruck, 6020 Innsbruck, Austria; philipp.zelger@i-med.ac.at (P.Z.)

3 Department of Radiology, Medical University of Innsbruck, 6020 Innsbruck, Austria; gerlig.widmann@i-med.ac.at (G.W.); hanna.kranebitter@student.ac.at (H.K.)

4 Department of Neuroradiology, Medical University of Innsbruck, 6020 Innsbruck, Austria; stephanie.mangesius@i-med.ac.at (S.M.)

5 Department of Radiation-Oncology, Medical University of Innsbruck, 6020 Innsbruck, Austria; julian.mangesius@i-med.ac.at (J.M.)

6 Department of Internal Medicine V (Hematology and Oncology), Comprehensive Cancer Center Innsbruck (CCCI), Medical University of Innsbruck, 6020 Innsbruck, Austria; florian.kocher@i-med.ac.at (F.K.)

* Correspondence: daniel.dejaco@i-med.ac.at; Tel.: 0043 504 512 23142

Simple Summary: Radiochemotherapy (RCT) in patients with locally advanced head and neck squamous cell carcinoma (HNSCC) causes side-effects in healthy tissue such as the sternocleidomastoid muscle (SCM). These side-effects depend on the interval between completion of RCT and restaging-CT. For salvage surgery, the optimal time window for surgery is postulated between 6 and 12 weeks, after completion of RCT. Thus, no extensive tissue fibrosis is to be expected. This interval is based on studies exploring surgical complications. Studies directly exploring radiation-induced changes of SCM in HNSCC-patients are sparse. This study applied radiomics to quantify radiation-induced changes in the SCM and paravertebral musculature (PVM). In 98 locally advanced HNSCC-patients, 3 radiomic key features (volume, mean-positivity-of-pixels, uniformity) were analyzed in CT-scans before and in the mean 8 weeks after treatment. No significant changes in radiomic key features were observed after adjustment for changes in body mass index (BMI). This data supports the postulated time window for salvage surgery of 6 to 12 weeks. Thus, additional surgical complications due to tissue fibrosis is not to be expected within this interval.

Abstract: Patients with locally advanced head and neck squamous cell carcinoma (HNSCC) frequently require primary radiochemotherapy (RCT). Despite intensity-modulation, desired radiation-induced effects observed in HNSCC, may also be observed as side-effects in healthy tissue e.g. the sternocleidomastoideus muscle (SCM). These side-effects (e.g. tissue fibrosis) depend on the interval between completion of RCT and restaging-CT. For salvage surgery, the optimal time window for surgery is currently postulated between 6 and 12 weeks after completion of RCT. Thus, no extensive tissue fibrosis is to be expected. This interval is based on studies exploring surgical

 doi:10.20944/preprints202309.0068.v1

complications. Studies directly exploring radiation-induced changes of the SCM in HNSCC-patients are sparse. The present study quantifies tissue alterations in SCM and paravertebral musculature (PVM) after RCT applying radiomics to determine the optimal time window for salvage surgery. Three radiomic key parameters 1) volume, 2) mean positivity of pixels (MPP) and 3) uniformity were extracted with mint lesion™ in the staging-CTs and restaging-CTs of 98 HNSCC-patients. Of these, 25 were female, the mean age was 62 (±9.6) years and 80.9% were UICC Stage IV. The mean restaging-interval was 55 (±28; range29-229) days. Only the mean volume significantly decreased after RCT from 9.0 to 8.4 and 96.5 to 91.9 ml for SCM and PVM, respectively (both $p=0.007$, both Cohen's $d=0.28$). In addition, the mean body mass index (BMI) decreases from 23.9 (±4.2) to 21.0 (±3.6) kg/m² ($p<0.001$); Cohen's $d = 0.9$). The mean BMI-decrease significantly correlated with the volume decrease for SCM ($r=0.27$; $p=0.007$) and PVM ($r=0.41$; $p<0.001$). If t-test p-values were adjusted for the BMI-decrease, no significant change in volumes for SCM and PVM was observed (both $p>0.05$). The present data supports the postulated optimal interval for salvage surgery of 6 to 12 weeks. Irrespective of the remaining risk-benefit ratio of salvage surgery, the risk of additional surgical complications due to fibrosis is not supported by the present observations.

Keywords: head and neck neoplasms; head and neck cancer; head and neck squamous cell carcinoma; radiotherapy; radiochemotherapy; salvage surgery; time interval; body composition; skeletal muscle; computed tomography scan; radiomics

1. Introduction

Most patients with locally advanced head and neck squamous cell carcinoma (HNSCC) require multimodality treatment [1, 2], frequently consisting of surgery followed by radiotherapy (RT) or primary concurrent radiochemotherapy (RCT) [3]. While the RT-part directly targets primary tumors and involved cervical lymph nodes, the chemotherapy-part aims at increasing radio-sensitivity and targets circulating tumor cells [2-4].

Modern photon-based radiation aims at primarily damaging primary tumors and suspicious cervical lymph nodes by more focused mechanisms almost exclusively at the site of radiation [5, 6]. Despite the introduction of three-dimensional and, conformal, intensity modulated radiation modalities, radiation-induced changes remains a challenge in RCT of HNSCC-patients [7]. Thus, direct and desired effects of radiation observed in cancer cells [6] may also be observed as undesired effects in otherwise healthy tissue, which lies adjacent to but is not infiltrated by HNSCC (e.g. salivary glands, mucosal membranes, or skeletal muscle) [5]. For skeletal muscle, these alterations are mediated via tissue or stem cell injury, cellular signal pathway alterations, and (epi)genetic changes [8-13]. In contrast, the chemotherapy of a primary RCT was not previously observed to induce similar and significant tissue alterations [3, 4].

The occurrence of these tissue alterations was previously discussed to depend on the interval between the end of RCT and the time of tissue assessment [14, 15]. During the first weeks after RCT, muscular inflammation was discussed to lead to interstitial edema [16]. In contrast, months after RCT a shift towards muscular fibrosis [14, 15] due misdirected wound healing [17, 18] can be observed. Thus, ultimately functional impairment may be observed [19-21].

Despite these functional impairments [19-21], this temporal dependence of tissue alterations after primary RCT also becomes relevant in the context of salvage surgery [22, 23]. Reports on the incidence of persistent primary tumors or cervical lymph nodes after primary RCT range from 22 up to 40% [24-26]. Irrespective of the risk-benefit ratio of salvage surgery after primary RCT (i.e. missing microscopic residual disease if not performed vs. probability of overtreatment if performed) with possible surgical complications, the optimal time window for salvage surgery is currently considered between 6 and 12 weeks after completion of primary RCT [27]. For this specific time window, no extensive tissues fibrosis and scarring was postulated, while acute adverse events of primary RCT have already subsided [27].

 doi:10.20944/preprints202309.0068.v1

Although various experts in the field currently consider this specific time window optimal, the definition of this interval is primarily based on studies exploring overall survival and surgical complications after salvage surgery [27]. To the best of our knowledge, no direct assessment of alterations of skeletal muscle composition in HNSCC-patients after primary RCT has been performed yet.

Currently, various methods exist to explore RT- and chemotherapy-induced alterations of skeletal muscle composition during and after RCT in HNSCC-patients [28]. Besides subjective methods such as palpation, which are more of historical relevance, objective methods to assess skeletal muscle composition in the neck were previously performed based on routinely acquired images during routine oncologic follow-up or small trials by using ultrasound or shear wave elastography [17, 18, 21, 29]. Despite these attempts, available data applying these methods to assess RT-induced alteration of skeletal muscle composition during and after RCT of HNSCC-patients are sparse.

No attempt has yet been made to explore short-term RCT-induced alterations of skeletal muscle composition after RCT in HNSCC-patients applying a radiomic approach [16-18, 21, 28, 29]. Radiomics is an emerging data-driven approach aiming at the extraction and processing of quantitative data to analyze image-based information [20]. The target is to treat medical imaging data of patients as data-minable sources for additional clinical information. The result can provide an ameliorated basis for the decision-making process [19].

The primary aim of this study was to quantify tissue alterations in skeletal muscles of the head and neck after primary RCT applying radiomic feature analysis on routinely acquired CT images, ultimately aiming at defining an optimal time window for salvage surgery in patients with persistent HNSCC after first line treatment.

2. Materials and Methods

2.1. Study population and additional clinical data

This retrospective cohort study adhered to the "Strengthening the Reporting of Observation studies in Epidemiology" (STROBE) guidelines [30]. From 2008 until 2021, patients of the institutional head and neck cancer registry at the Department of Otorhinolaryngology, Head and Neck Surgery, Medical University of Innsbruck, Austria, that had 1) incident, histologically confirmed, locally advanced HNSCC (UICC III or IV), 2) who were treated with primary RCT and 3) for whom contrast-enhanced computed tomography scans before treatment ("staging-CT") and after treatment ("restaging-CT") were available, were eligible.

From 1,110 potentially eligible patients, 840 did not meet the inclusion criteria. From the remaining 270 patients, 25 have been excluded due to insufficient quality (e.g., dental artifacts) of the contrast-enhanced computed tomography scan (CT) prior to primary RCT ("staging-CT") and/or after primary RCT ("restaging-CT) (n=10), unavailability of either of the two imaging modalities (n=13) or SCM radiation dose <49 Gy. Of the remaining 245 patients, a representative random sample was drawn with SPSS 28 (IBM, Armonk, NY, USA). The study flow diagram and patient inclusion modified according to Standards for Reporting Diagnostic accuracy studies criteria (STARD) [31] is depicted in Figure 1.

Preprints (www.preprints.org) | NOT PEER-REVIEWED | Posted: 4 September 2023 doi:10.20944/preprints202309.0068.v1

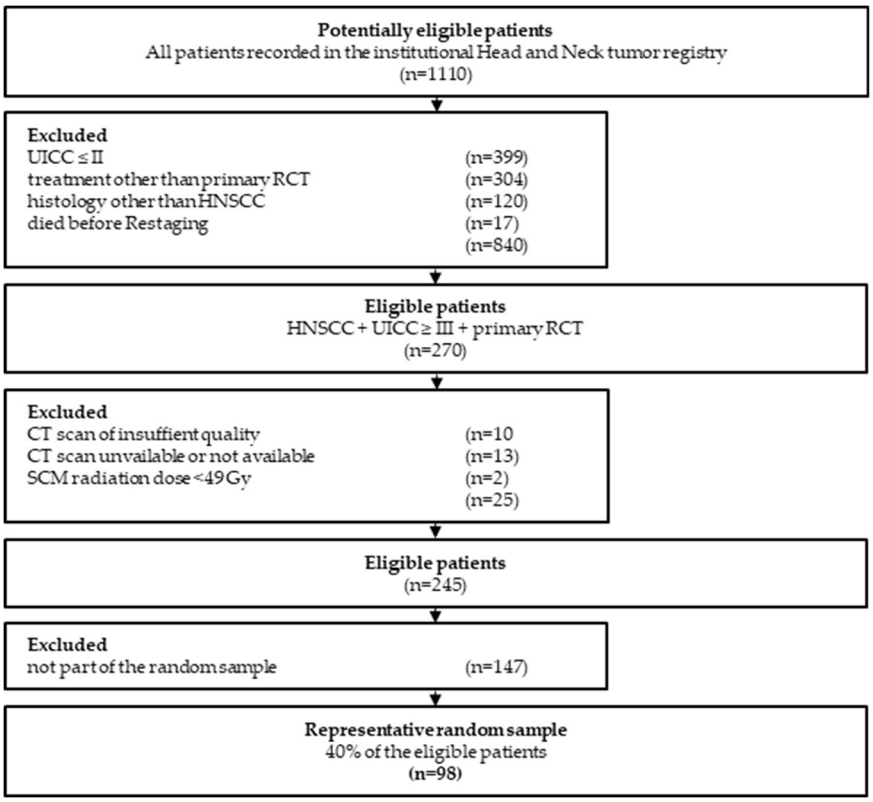

Figure 1. Study flow and patient inclusion modified according to STARD criteria [31]. A total of 1,100 patients were potentially eligible, of which 840 did not meet the inclusion criteria. Of 270 eligible patients, 23 were excluded due to insufficient quality of the contrast-enhanced CT-scan (e.g. dental artifacts) and 13 due to unavailability of either of the two imaging modalities. A representative random sample of 98 patients was drawn. The clinical characteristics of the 98 included patients are presented in Table 2.

2.2. Clinical data

Clinical data has been extracted from the institutional head-and-neck cancer registry or the electronic hospital information system (PowerChart, Cerner, Kansas City, MI, USA) including age, gender, year of first diagnosis, tumor site, UICC stage, date of the CT scans, alcohol consumption, smoking, Radiation dose, p16 status, body mass index (BMI), serum protein level, American Association of Anesthesiologists (ASA) score and functional outcome.

2.3. CT imaging acquisition

Staging and restaging contrast-CTs adhered to the head and neck CT imaging protocols of the Department of Radiology (Medical University of Innsbruck, Austira) and were acquired with a Light Speed VCT or a Light Speed 16 CT scanner (GE Medical Systems, Vienna, Austria). The scan volume ranged from the skull base to the upper mediastinum with a resolution of 512×512 pixels, 2 mm slice thickness, collimation of 24 × 1.2 mm, and 0.45 pitch. Sagittal and coronal images were reconstructed from the axial images. As a contrast agent, Jopamiro 370 (Bracco Austria GmbH, Vienna, Austria) was administered intravenously adjusted to the patient's body weight. Staging- and restaging contrast CTs used the same protocols, making the studies of each patient comparable.

2.4. Segmentation of head-and-neck musculature

All staging and restaging-CTs were first exported to Digital Imaging and Communications in Medicine format using the IMPAX EE image archiving and communication system (Agfa HealthCare, Bonn, Germany). Thereafter, the images were exported and further processed using mint Lesion™

 doi:10.20944/preprints202309.0068.v1

(Mint Medical GmbH, Heidelberg, Germany, version 3.8.1). For each patient, both sternocleidomastoideus muscles (SCM) and the paravertebral musculature (PVM) including the following muscles: trapezius, longus capitis, splenius capitis, semispinalis capitis, longissimus capitis, levator scapulae, longus colli, were segmented in staging- and restaging-CT.

The SCM, in the field of radiation and additionally affected by scatter-irradiation, was chosen to explore RT-induced alterations, while the PVM, primarily affected by chemotherapy and less by scatter-irradiation, was chosen to explore chemotherapy-induced alterations.

Segmentations were performed manually in all data-sets slice by slice in axial planes using the "paint on slices" tool provided by the software from the upper edge to the lower edge of the 3rd cervical vertebra. This approach was previously proposed to be effective in the assessment of head-and-neck musculature in HNSCC-patients [32].

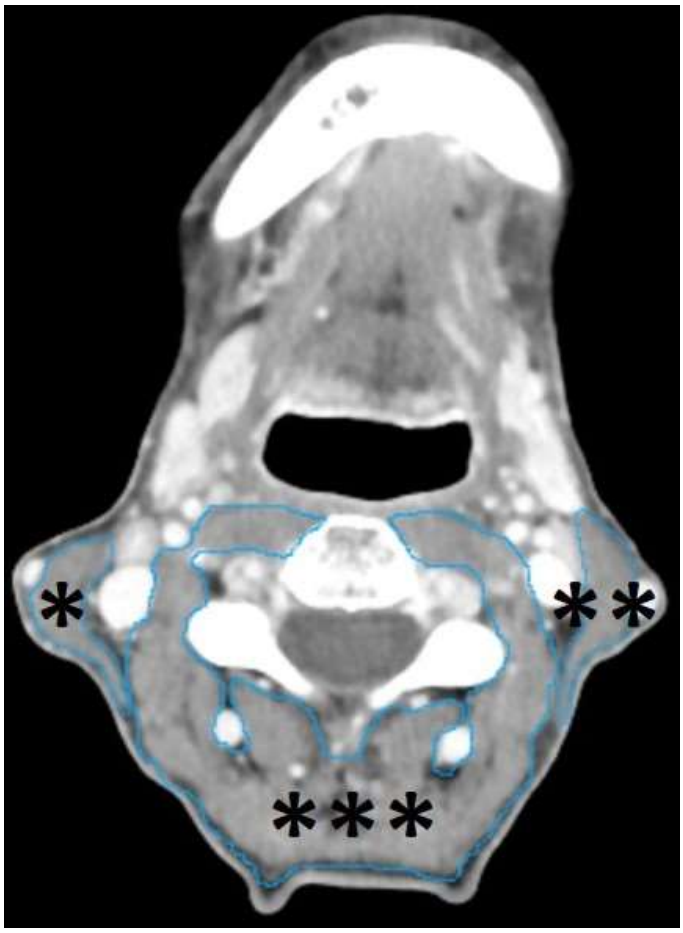

Figure 2. Example of segmented head-and-neck musculature in a staging-CT of a 56-year-old, male HNSCC-patients with a tumor of the hypopharynx (not depicted) staged cT3 cN0 cM0. The manual slice by slice segmentation was performed in the axial plane using the "paint on slice" tool provided by mint Lesion™ (Mint Medical GmbH, Heidelberg, Germany, version 3.8.1) at the level of the 3rd cervical vertebra, as previously proposed [32], for the right SCM (*), the left SCM (**) and the PVM (***), which includes the following muscles: trapezius, longus capitis, splenius capitis, semispinalis capitis, longissimus capitis, levator scapulae, longus colli.

2.5. Data analysis

At the time this study was conducted, mint Lesion™ provided 13 radiomic parameters for the 3 segmented muscle groups SCM right, SCM left, and PVM each before and after therapy. Normally distributed data were described by mean and standard deviation, and non-normally distributed

 doi:10.20944/preprints202309.0068.v1

parameters were described by median and 25th and 75th percentiles. Frequencies were tabulated and presented with percentages.

To reduce the number of radiomic parameters (initially 13), a principal component analysis (PCA) with varimax rotation was performed. Here, 3 components could be extracted. Attempts with more components did not yield better results. The 3 extracted components were: 1) volume, 2) mean pixel positivity (MMP) and 3) uniformity. Volume in milliliters (ml) represents the spatial dimension of the segmented muscles SCM and PVM. A change in volume was considered as surrogate for loss of musculature (i.e. sarcopenia) or inflammation and interstitial edema. Mean positivity of pixels (MPP) in Hounsfield-units (HU), represents an intensity parameter, which is a dimensionless absolute number. A change in MPP was considered as surrogate for fibrosis (i.e. increase) or edema (i.e. decrease). Uniformity, a dimensionless absolute number, represents the texture of the segmented muscles SCM and PVM. A change in uniformity was considered as surrogate for changes in texture (i.e fibrosis or edema).

These components had high loadings for the output values of volume, MPP, and uniformity provided by mint Lesion™ (Table 1; all >0.9.). Therefore, these 3 original values provided by mint Lesion™ were used for the present analyses. The remaining 10 radiomic parameters provided by mint Lesion™ correlated closely with one of these 3 radiomic features each. Thus, they were largely redundant and were not considered in further analysis.

Table 1. All 13 individual radiomic features and their corresponding radiomic key feature extracted with mint Lesion™ (Mint Medical GmbH, Heidelberg, Germany, version 3.8.1).

Radiomic key features	Individual radiomic features
Shape features	Short axis diameter[1]
	Long axis diameter[1]
	Volume[2]
Texture features[3]	Entropy
	Uniformity
Intensity features[3]	Maximal density
	Minimal density
	Mean density
	Skewness of density
	Standard deviation of density
	MPP
	Uniformity of distribution of positive pixels (UPP)
	Kurtosis

[1]Diameters are provided in millimeters; [2]volumes are provided in milliliters; [3]all texture and intensity features are provided without dimension.

These three key features represented the spatial dimensions, pixel intensity, and pixel uniformity of the segmented muscles.

The values of the 3 radiomic parameters volume, MPP and uniformity were available for each of the 3 muscle groups (SCM left, SCM right, PVM) before and after therapy. Only the SCM data of the irradiated side were evaluated; if the radiation dose was the same on the right and left sides, the right SCM was used. PVM was omitted from the radiation field and received the lowest possible radiation dose. The radiation dose to the irradiated SCM and the interval between diagnostic CT and restaging-CT were recorded. In addition, data on BMI and serum protein level before and after therapy were available.

First, we tested for linear correlations (Pearson) between values before therapy for the radiomic parameters volume, MPP, uniformity, and patient age, BMI, and serum protein level. The influence of gender, tumor site, UICC-stage, general health as measured by ASA score (I/II vs. III/IV), smoking

 doi:10.20944/preprints202309.0068.v1

status (<= or > 10 packyears), and alcohol consumption (daily or less frequently than daily) on pretherapeutic parameters was examined by variance analysis.

The differences before and after therapy for the parameters volume, MPP, uniformity, BMI, and serum protein level were tested with the paired-samples T test (two-sided). Cohens' d with Hedges correction was used as the effect size parameter. For further mechanistic analyses, the differences after therapy minus before therapy were calculated for these data and subjected to bivariate parametric correlation analyses and variance analysis. In addition, for the radiomic parameters, the results of the paired T tests were adjusted for the effect of BMI difference by including BMI difference as a covariate.

2.6. Ethical considerations

The study has been approved by the review board of the Medical University of Innsbruck, Austria (1269/2018). All procedures conducted in these studies involving human participants are in accordance with the ethical standards of the institutional review board and with the Helsinki declaration (1964) and its later amendments or comparable ethical standards.

3. Results

3.1. Patient population

A total of 1,110 patients recorded in the institutional HNC registry were potentially eligible. Of these, 853 were excluded as they met one or more of the exclusion criteria (Figure 1). After drawing a representative random sample of the remaining 247 patients, 98 patients were included in this study.

Of these, 73 (74.5%) were male and 25 (25.5%) were female. Mean age at initial diagnosis was 62.0 (± 9.6) years ranging from 42 to 81 years. Of the included 98 patients, the tumor site was oropharynx in 46 (46.9%), hypopharynx in 20 (20.4 %), larynx in 15 (15.3%), oral cavity in 13 (13.3%), and other site in 4 (4.1%) patients. Of the 46 patients diagnosed with oropharyngeal HNSCC, 29 (63.0%) were categorized as p16 positive, using immunohistochemistry with a positivity cut-off of 60%. A total of 93 (94.9%) patients had a UICC Stage III-IV and 5 (5.1%) a UICC stage I-II. HNSCC.

In terms of comorbidities, 53 (54.1%) patients were classified as ASA III/IV and 45 (45.9%) as ASA I/II. All 98 (100.0%) included patients were smokers and 52 patients (53.1%) drank alcohol daily; the remaining 46 patients (46.9%) did not drink daily. BMI data were collected from 79 (80.6%) patients at initial diagnosis. The mean BMI was 24.2 (± 4.9) ranging from 13.8 to 47.7. Thus, 7 (8.9%) patients are underweighted, 41 were (51.9%) normal weighted, 25 (31.6 %) were overweighed and 6 (7.6%) were defined as adipose. Additional detail about clinical characteristics of the 98 included HNSCC-patients is provide in the following table (Table 2).

Table 2. Clinical characteristics of the 98 included HNSCC-patients.

		Number	Percentages
Sex	Male	73	74.5%
	Female	25	25.5%
Age	≤50	11	11.2%
	51-60	35	35.7%
	61-70	33	33.7%
	≥71	19	19.4%
Tumor site	Oral cavity	13	13.3%
	Oropharynx	46	46.9%
	Hypopharynx	20	20.4%
	Larynx	15	15.3%
	Others	4	4.1%
UICC[1] truncated	Stage III	19	19.4%

Preprints (www.preprints.org) | NOT PEER-REVIEWED | Posted: 4 September 2023 doi:10.20944/preprints202309.0068.v1

	Stage IV	79	80.6%
ASA	ASA I/II	45	45.9%
	ASA III/IV	53	54.1%
Alcohol consumption	< daily	52	53.1%
	daily	46	46.9%
Smoking habits	< 10 PY	24	24.5%
	≥ 10 PY	74	75.5%
BMI-classified	Underweight	7	8.9%
	Normal weight	41	51.9%
	Overweight	25	31.6%
	Adipose	6	7.6%
Radiation dose[1]	≤60 Gy	26	26.5%
	>60 Gy	72	73.5%

[1]Dosage in Gy on the investigated SCM.

3.2. Primary radiochemotherapy and time intervals

All 98 included HNSCC-patients were treated with primary RCT. Of these, 72 patients (73.5%) received a radiation dosage greater than 60 gray (Gy), 26 patients (26.5%) received 60 Gy or less on the irradiated SCM. Means, standard deviation and range for the imaging interval (i.e. interval between staging-CT and restaging-CT) and restaging interval (i.e. interval between end of primary RCT and restaging-CT) are provided in Table 3 (Table 3).

Table 3. Time intervals of the 98 included HNSCC-patients between staging-CT and restaging-CT (imaging interval) as well as between end of RCT and restaging- CT (restaging interval).

	Mean (days)	**Minimum (days)**	**Maximum (days)**	**Standard Deviation (days)**
Imaging interval[1]	148	108	315	±33
Restaging interval[2]	55	29	229	±28

[1]Imaging interval: interval between staging-CT and restaging-CT in days; [2]Restaging-interval: interval between end of RCT and restaging-CT in days.

3.3. Variable reduction (principal component analysis)

For dimensional reduction of the radiomic parameters yielded by mint Lesion™, a PCA with varimax rotation was performed. From the 13 parameters of mint Lesion™, 3 principal components could be extracted. The 3 extracted components via PCA explained more than 70% of the variance of the values and were uncorrelated (Appendix 1). The Kaiser-Meyer-Olkin Measure of Sampling Adequacy was 0.61 indicating an acceptable sampling adequacy.

The component matrix allows the interpretation of the 3 extracted components based on their factor loadings (Appendix 2). The first component represents a measure of uniformity of pixels in the segmented muscle, which is inversely correlated with entropy. The second component represents a measure of pixel intensity and the third component represents a measure of spatial dimension.

3.4. Factors influencing pretherapeutic Volume, uniformity and MPP

For comparisons, the right SCM was used as reference for the 3 segmented muscle groups. A correlation (Pearson) between muscle volume, BMI ($r= 0.56$; $p<0.001$) and serum protein level ($r=0.31$; $p=0.002$) before therapy was observed. In addition, a weak inverse correlation between uniformity and age was observed ($r= -0.21$; $p=0.035$).

Further comparisons (independent t-tests) revealed differences in gender. Pretherapeutic SCM volume on the right was 10.0 (±2.8) ml in 73 men and 5.9 (±1.7) ml in 25 women ($p<0.001$). Differences

 doi:10.20944/preprints202309.0068.v1

according to gender were also observed for MPP, 58.8 (±7.9) in men and 63.0 (±9.1) in women (p=0.014), while there were no gender differences for uniformity. The other demographic and clinical factors (UICC stage, general health status (ASA-score), smoking status (<10

Py/>10Py) or alcohol consumption (daily or less frequently) did not affect the radiomic parameters explored.

3.5. Volume, uniformity and MPP before and after therapy

The radiomic parameters for the SCM on the irradiated side of the neck that was exposed to the full radiation dose did not change except for volume (Table 4). Volume showed a decrease from 9.00 (±3.2) to 8.4 (±2.7) ml (p=0.007), with a Cohen's d of 0.28 indicating a weak effect.

Table 4. Radiomic key parameters extracted via mint Lesion™ in staging-CTs (i.e. pretreamtent) and approximately 21 weeks later in restaging-CTs (i.e. posttreatment) in included 98 patients with incident, locally advanced HNSCC.

Radiomic key features	Staging-CT (SD)	Restaging-CT (SD)	p-value[1]	Cohen's d[2]
SCM-Volume (ml)	9.00 (±3.2)	8.4 (±2.7)	0.007	0.28
SCM-MPP (HU)	60.1 (±8.7)	59.7 (±8.1)	0.664	0.04
SCM-Uniformity*	16.8 (±4.3)	16.4 (±4.1)	0.342	0.10
PVM –Volume (ml)	96.5 (±30.2)	91.9 (±25.8)	0.007	0.28
PVM –MPP (HU)	56.3 (±8.6)	58.0 (±8.6)	0.061	-0.19
PVM –Uniformity*	11.6 (±3.1)	12.0 (±2.8)	0.058	-0.19

[1]two-sided paired sample t-Test; 2Cohen's D with Hedges correction; *values provided multipled with 1000;SD: standard deviation.

The SCM, in the field of radiation and additionally affected by scatter-irradiation, was chosen to explore RT-induced alterations, while the PVM, primarily affected by chemotherapy and less by scatter-irradiation, was chosen to explore chemotherapy-induced alterations.

The PVM, primarily affected by chemotherapy and less by scatter-irradiation, was chosen to explore primarily for chemotherapy associated muscular changes. However, changes analogous to those in the SCM were observed. The volume decreased from 96.5 (±30.2) to 91.9 (±25.8) (p=0.007; Cohen's d = 0.28). MPP and uniformity showed trends toward increase but may be due to chance (p>0.05, Table 4). Since the PVM were outside the radiation field, direct radiation exposure cannot explain the observed volume decreases.

Consequently, it was tested whether the volume difference correlates with other parameters. Significant changes before and after therapy were seen in BMI with a decrease from 23.9 (±4.2) to 20.98 (±3.59) kg/m² (p=<0.001; Cohen's d = 0.9) and serum protein levels decreased from 7.4 (±0.53) to 6.75 (±0.85) mg/% (p<0.001; Cohen's d 0.7). Therefore, Pearson correlation analyses were included between volume differences before and after therapy and BMI difference, as well as difference in serum protein levels before and after therapy. First, there was a significant correlation of the volume differences of SCM and PVM (r=0.58; p<0.001). In addition, volume decrease of SCM and decrease of BMI correlated (r=0.27; p=0.007) as well as volume decrease of PVM musculature and BMI decrease (r=0.41; p<0.001). The decrease in serum protein levels did not correlate with the explored radiomic key parameters.

To test whether the radiomic volume decreases were due to the decrease in BMI, the results of the t-tests were adjusted for the difference in BMI values. For this purpose, general linear models completely analogous to the paired t-tests were used, with the BMI difference as a covariate. Here, the irradiated SCM showed a significant interaction between volume and BMI decrease (p=0.007), whereas the difference before/after therapy was no longer significant (p=0.9). Similarly, PVM showed a significant interaction of volume decrease with BMI decrease (p<0.001) and the volume decrease before/after therapy was no longer significant (p=0.71).

4. Discussion

Multimodality treatment is frequently required in the treatment of locally advanced HNSCC [1-4]. Despite the precision of modern RT, which primarily targets the primary tumor and suspect cervical lymph nodes [5, 6], undesired tissue alterations (i.e fibrosis) especially in skeletal muscle of the head and neck were previously observed [14-18]. These alterations occurs in musculature, which was directly in the field of radiation (i.e. SCM) but also in musculature, which was only indirectly affected by scatter irradiation (i.e. PVM) [14-18].

A link between the observed tissue alterations and the time interval between end of RCT and the time of tissue assessment was previously postulated [14, 15]. This postulated temporal linkage is of crucial importance in the context of salvage surgery, which is frequently necessary in the context of tumor or lymph node persistency after RCT [22-26]. The optimal time window to perform salvage surgery was previously postulated by experts in the field between 6 and 12 weeks after the completion of RCT [27]. For this specific time window no extensive tissues fibrosis and scarring has to be expected, while acute adverse events of primary RCT have already subsided [27].

Unfortunately, the definition of this specific time window for salvage surgery was mainly based on studies exploring overall survival and surgical complications after salvage surgery [27]. Studies that directly assess tissue alterations in skeletal muscle of the head and neck after RCT are sparse [17, 18, 21, 29]. To the best of our knowledge, no attempt has yet been made to explore short-term RCT-induced alterations of skeletal muscle after RCT in HNSCC-patients applying radiomics, a data-driven approach aiming at the extraction and processing of quantitative data to analyze image-based information [19, 20].

The primary aim of this study was to quantify tissue alterations in skeletal muscles of the head and neck after primary RCT applying radiomic feature analysis, ultimately aiming at defining an optimal time window for salvage surgery in patients with persistent HNSCC after first line treatment.

From a total of 247 eligible patients with locally advanced HNSCC recorded in the institutional HNC registry, a representative sample of 98 patients was drawn. Of these 98 patients, common clinical characteristics including sex, age, tumor site, p16 status, smoking and drinking habits were comparable with previous, larger cancer registry based studies [33] (Table 2). Thus, the sample drawn from the originally 247 eligible patients appears representative.

The imaging interval (i.e. the time between the pretreatment staging-CT and the posttreatment restaging-CT) was approximately 21 weeks, ranging from 15 weeks to 45 weeks (Table 3). In this specific interval diagnostic work-up, interdisciplinary tumor board presentation and pretreatment procedures including dental treatments and application of percutaneous gastrostomies were carried out. At our institution this pretreatment procedures prior to the start of primary RCT requires approximately 3 to 4 weeks and primary RCT an additional 6 to 8 weeks. Restaging was performed 6 to 12 weeks after end of RCT. Thus, without complications during pretreatment procedures (e.g. percutaneous gastrostomy wound infections) or during primary RCT (e.g. postponing a radiochemotherapy cycle due to changes in white blood count), this interval ranges from 15 to 24 weeks. In the present study, the maximum interval observed was approximately 45 weeks. In this specific patient a combination of pre- (peritonitis after percutaneous gastrostomy) and intratreament complications (multiple postponing of radiochemotherapy cycles due to neutropenia) occurred.

The restaging interval (i.e. the time between end of the RCT and the restaging-CT) was approximately 8 weeks, ranging from 4 weeks to 33 weeks (Table 3). Thus, the mean time interval of the population explored in this study is in line with the recommended restaging interval, if additional salvage surgery is required [27]. The patient with the shortest restaging interval of 29 days was diagnosed with cT4a cN3b cM0 laryngeal cancer and therefore required urgent salvage laryngectomy. Thus a considerably shorter restaging interval was observed for this patient. The patient with the longest restaging interval of 229 days, was the one patient with multiple pre- and intratreatment complications, which required a prolonged intensive care unit stay after completion of the primary RCT.

In summary, the intervals observed in the present study appear in line with intervals reported in previous studies [34-36]. Consequently, the observations of this study may be applied to the

 doi:10.20944/preprints202309.0068.v1

postulated optimal time window to perform salvage surgery by experts in the field between 6 and 12 weeks after the completion of RCT [27].

The first key finding of the present study was that volume was the only radiomic key parameter, which was subject to significant change after primary RCT. The mean SCM-volume decreased from 9.0 to 8.4 ml and the PVM-volume from 96.5 to 91.9 ml (both $p=0.007$). Some crucial aspects of this observation need to be discussed: considering the restaging interval of approximately 8 weeks (Table 3), an increase in volume due to muscular inflammation and interstitial edema in the SCM, directly affected by irradiation, was to be expected [16]. In addition, a significant decrease in mean PVM-volumes was observed, which is primarily affected by chemotherapy but not by irradiation.

Consequently, it was considered unlikely that these observed changes in volume were primarily caused by irradiation, chemotherapy or the combination of the both treatment modalities alone. Moreover additional, significant decreases in mean BMI from 23.9 to 21.0 kg/m² and in mean serum protein levels from 7.4 to 6.6 mg/% (both $p<0.001$) were observed. These two parameters were included in Pearson correlation analyses, which revealed a significant and strong correlation for the BMI decrease ($p<0.001$; $r=0.41$). In a last step, the original results of the t-test applied to the volumetric changes were adjusted for the difference in BMI values ultimately resulting in insignificant volume changes for SCM and PVM after treatment (both $p>0.05$). Other studies, such as Choi et al., came to a similar conclusion. However, in the aforementioned work, the method of measurement differed and contained significantly fewer parameters [37-40].

Thus, the second key finding of the present study was that no significant changes in the explored radiomic key features was observed, if adjusted for changes in BMI before and after treatment. This observation has several implications.

Firstly, this observation highlights the importance of optimal assessment and optimization of nutrition before, during and after primary RCT. Regular assessments of nutritional status and BMI before, during and after primary RCT for HNSCC-patients was previously recommended by other authors [41].

Secondly, the data of the present study supports the previously postulated optimal time window to perform salvage surgery [27]. Neither did the volume of the muscles explored significantly change, if corrected for changes in BMI, nor did the radiomic key features MMP and uniformity, which can be considered as surrogates for tissue fibrosis. Thus, irrespective of the remaining risk-benefit ratio of salvage surgery after primary RCT (i.e. missing microscopic residual disease if not performed vs. probability of overtreatment if performed), the risk of additional surgical complications due to tissue fibrosis or volumetric change in the head and neck musculature is not supported by the present data.

Certain limitations of the present study need to be addressed. Firstly, this comparatively small numbered retrospective study exploring only patients with advanced-stage HNSCC should be supplemented by a larger, prospective investigation. Secondly, various data processing programs are available to segment anatomical structures. For the present study the commercially available software mint Lesion™ was chosen due to the advantage of providing a structured, standardized feature output available to everyone, which minimizes the risk of bias. However, at the time of the study, only 13 radiomic features were routinely extracted by mint Lesion™. Furthermore, these 13 features were reduced to three key features via PCA. Although, applying machine learning or deep neural networks for statistical analysis, attempts with more components did not yield better results [42]. Thirdly, the time interval chosen for the present study only explored for short-term radiomic changes with a mean restaging interval of approximately 8 weeks. An expansion of this observation interval to months or years would be crucial to assess whether previously proposed changes of head and neck musculature due to primary RCT can be detected by the means of a radiomic approach.

5. Conclusions

After a mean interval of approximately 8 weeks after completion of primary RCT, no significant radiomic changes could be assessed. The data of the present study supports the previously postulated optimal time window to perform salvage surgery of 6 to 12 weeks. Thus, irrespective of the remaining risk-benefit ratio of salvage surgery after primary RCT (i.e. missing microscopic residual disease if

Preprints (www.preprints.org) | NOT PEER-REVIEWED | Posted: 4 September 2023 doi:10.20944/preprints202309.0068.v1

not performed vs. probability of overtreatment if performed), the risk of additional surgical complications due to tissue fibrosis or volumetric change in the head and neck musculature is not supported by the present data.

Author Contributions alphabetically ranked by surname: Idea, D.D., G.W. and H.R.; conceptualization, D.D., W.F., H.K., J.M., A.R., M.S.; methodology, D.D., G.W. and H.R.; formal analysis, T.M.G., F.K. P.Z.; investigation, D.D., H.K., H.R., M.S.; data curation, D.D., H.K., H.R., M.S.; writing—original draft preparation, reviewing and editing, D.D., B.H., J.S., H.R., M.S.; supervision, D.D., B.H., J.S., H.R.; project administration, D.D., S.M. and H.R. All authors have read and agreed to the published version of the manuscript.

Funding: This research received no external funding.

Institutional Review Board Statement: The study was conducted according to the guidelines of the Declaration of Helsinki and approved by the Institutional Ethics Committee of the Medical University of Innsbruck, Austria (1269/2018).

Informed Consent Statement: Informed consent was obtained from all subjects involved in the study.

Data Availability Statement: The data presented in this study are available on request from the corresponding author.

Conflicts of Interest: The authors declare no conflict of interest.

Appendix

Appendix 1: Descriptive statistics of the original obtained values by mint Lesion™ for the SCM and PVM. In addition, the Data fort the SCM of the radiated side (SCM-rad) are provided. These data were obtained before treatment.

	N	Minimum	Maximum	Mean	Standard deviation
SCMright_Short_Axis	98	4.7	24.3	14.251	3.4045
SCMright_Long_Axis	98	19.5	60.9	42.026	7.5338
SCMright_Volume	98	3.3	17.8	8.971	3.1417
SCMright_Entropy	98	5.5	7.3	6.489	0.3232
SCMright_Kurtosis	98	3.1	24.4	6.557	2.7009
SCMright_MPP	98	31.6	79.2	59.880	8.3491
SCMright_Density_Max.	98	72	234	137.21	36.768
SCMright_Density_Min.	98	-155	-66	-105.32	17.386
SCMright_Density_Mean	98	23.8	77.5	51.176	10.9033
SCMright_Density_Skewness	98	-3.0	-1.0	-1.75	0.373
SCMright_Density_SD	98	13.9	45.3	32.183	5.9952
SCMright_UPP	98	0.0076	0.0298	0.016484	0.0041614
SCMright_Uniformity	98	0.0078	0.0298	0.016621	0.0040749
SCMleft_Short_Axis	98	5.0	27.7	14.547	3.7930
SCMleft_Long_Axis	98	23.8	57.5	42.623	7.6126
SCMleft_Volume	98	2.9	15.7	8.930	3.0336
SCMleft_Entropy	98	5.5	7.3	6.494	0.3395
SCMleft_Kurtosis	98	2.0	14.6	6.262	2.0012
SCMleft_MPP	98	37.1	86.0	59.344	8.4566
SCMleft_Density M_Axis	98	73	200	138.57	28.363
SCMleft_Density_Min.	98	-178	-48	-105.65	18.427
SCMleft_Density_Mean	98	23.6	78.6	50.546	10.9604
SCMleft_Density_Skewness	98	-3.4	-0.8	-1.717	0.4310
SCMleft_Density SD	98	14.1	47.9	32.052	6.5302
SCMleft_UPP	98	0.0075	0.0291	0.016344	0.0043101
SCMleft_Uniformity	98	0.0078	0.0291	0.016514	0.0042213

Preprints (www.preprints.org) | NOT PEER-REVIEWED | Posted: 4 September 2023 doi:10.20944/preprints202309.0068.v1

PVM_Short_Axig	98	43.7	88.9	66.209	10.0206
PVM_Long _Axis	98	63.3	176.3	100.281	18.8547
PVM_Volume	98	34.4	183.9	96.452	30.1608
PVM_Entropy	98	5.9675	7.5142	6.959589	0.2929190
PVM_Kurtosis	98	1.20	32.40	7.1407	4.72660
PVM_MPP	98	34.9	77.2	56.324	8.6289
PVM_Density_Max.	98	220.0	1278.0	520.678	211.4958
PVM_Density Min.	98	-198	-86	-127.35	19.423
PVM_Density_Mean	98	11.9	70.0	43.765	12.7727
PVM_Density_Skewness	98	-2.1	3.0	-0.735	0.8544
PVM_Density_SD	98	20.1	61.8	39.053	7.0062
PVM_UPP	98	0.0057	0.0235	0.011340	0.0032782
PVM_Uniformity	98	0.0067	0.0235	0.011584	0.0030456
SCM-rad_Volume	98	3.30	17.80	8.9992	3.15632
SCM-rad_Entropyopy	98	5.45	7.28	6.4731	0.33946
SCM-rad_MPP	98	31.60	86.00	60.1269	8.70200
SCM-rad_Density Mean	98	23.60	78.60	51.9051	11.08669
SCM-rad_Uniformity	98	0.01	0.03	0.0168	0.00425

Appendix 2: Matrix of observed Pearson correlation coefficients (here: right SCM); n=98; bold numbers indicate correlation coefficients between +/- 0.5 and +/- 0.99.

	Short _Axis	Long _Axis	Volume	Entropy	Kurtosis	MPP	Density_Max.	Density_Min.	Density_Mean	Density_Skewness	Density_SD	UPP	Uniformity
Short _Axis	1.00	0.11	0.45	-0.12	0.12	0.06	0.00	0.04	0.13	-0.12	-0.16	0.10	0.09
Long _Axis	0.11	1.00	**0.72**	-0.09	0.12	-0.03	0.04	-0.04	0.01	-0.13	-0.07	0.10	0.10
Volume	0.45	**0.72**	1.00	-0.12	0.13	-0.06	-0.03	-0.07	-0.01	-0.16	-0.12	0.12	0.11
Entropy	-0.12	-0.09	-0.12	1.00	**-0.72**	-0.04	0.28	**-0.58**	-0.37	**0.70**	**0.87**	**-0.96**	**-0.96**
Kurtosis	0.12	0.12	0.13	**-0.72**	1.00	0.27	0.02	0.18	0.46	**-0.76**	**-0.57**	**0.75**	**0.75**
MPP	0.06	-0.03	-0.06	-0.04	0.27	1.00	0.35	0.22	**0.90**	-0.11	0.06	0.12	0.11
Density M _Axis	0.00	0.04	-0.03	0.28	0.02	0.35	1.00	-0.13	0.27	0.24	0.18	-0.25	-0.25
Density Min	0.04	-0.04	-0.07	**-0.58**	0.18	0.22	-0.13	1.00	0.47	-0.01	**-0.68**	0.48	0.47
Density Mean	0.13	0.01	-0.01	-0.37	0.46	**0.90**	0.27	0.47	1.00	-0.25	-0.35	0.38	0.36
Density Skew	-0.12	-0.13	-0.16	**0.70**	**-0.76**	-0.11	0.24	-0.01	-0.25	1.00	0.40	**-0.76**	**-0.76**
Density STD	-0.16	-0.07	-0.12	**0.87**	**-0.57**	0.06	0.18	**-0.68**	-0.35	0.40	1.00	**-0.73**	**-0.72**
UPP	0.10	0.10	0.12	**-0.96**	**0.75**	0.12	-0.25	0.48	0.38	**-0.76**	**-0.73**	1.00	1.00
Uniformity	0.09	0.10	0.11	**-0.96**	**0.75**	0.11	-0.25	0.47	0.36	**-0.76**	**-0.72**	1.00	1.00

Appendix 3: Data variance explained by the 3 extracted factors.

Component	Sums of Squared Loadings	% of Variance	Cumulative %
Uniformity	5.3	40.8	40.8
Intensity	2.2	16.6	57.4
Dimension	2.0	15.2	72.6

Appendix 4: Matrix of the three extracted components and the rotated factor loadings of the initial parameters. Principal component analysis, Varimax rotation with Kaiser normalization.

Factor loadings	Uniformity	Intensity	Dimension
Entropy	-0.99		

Preprints (www.preprints.org) | NOT PEER-REVIEWED | Posted: 4 September 2023 doi:10.20944/preprints202309.0068.v1

UPP	0.97		
Uniformity	0.97		
Density SD	-0.84		
Kurtosis	0.77		
Density Skewness	-0.74		
Density Min.	0.57		
MPP		0.94	
Density Mean	0.41	0.88	
Density Max.	-0.31	0.62	
Volume			0.93
Long_Axis			0.82
Short_Axis			0.54

Appendix 5: Pearson correlation coefficients [r] and according two-sided probabilities (p) between the 3 components (factors) obtained by principal component analysis and the original parameters obtained by mint Lesion™ with high factor loadings. For simplicity, these 3 original parameters were used instead of the 3 components.

		Dimension-Factor	Uniformity-Factor	Intensity-Factor	Original Volume	Original Uniformity	Original Intensity (MPP)
Dimension-Factor	r	1	0.08	0.017	0.937	0.165	0.018
	p		0.435	0.865	0.001	0.104	0.858
Uniformity-Factor	r		1	0.268	0.075	0.966	0.317
	p			0.008	0.462	0.001	0.001
Intensity-Factor	r			1	-0.074	0.228	0.963
	p				0.468	0.024	0.001
Original Volume	r				1	0.155	-0.057
	p					0.127	0.575
Original Uniformity	r					1	0.284
	p						0.005
Original Intensity (MPP)	r						1
	p						

References

1. Chow, L.Q.M. Head and Neck Cancer. *N Engl J Med*. **2020.** 382(1): p. 60-72. doi: 10.1056/NEJMra1715715.
2. Machiels JP; René Leemans C; Golusinski W; Grau C; Licitra L; Gregoire V. Squamous cell carcinoma of the oral cavity, larynx, oropharynx and hypopharynx: EHNS-ESMO-ESTRO Clinical Practice Guidelines for diagnosis, treatment and follow-up. *Ann Oncol*. **2020**, 31(11): p. 1462-1475. doi: 10.1016/j.annonc.2020.07.011.
3. Kanno Y; Chen CY; Lee HL; Chiou JF; Chen YJ. Molecular Mechanisms of Chemotherapy Resistance in Head and Neck Cancers. *Front Oncol*. **2021**. 11: p. 640392. doi: 10.3389/fonc.2021.640392
4. Maloney SM; Hoover CA; Morejon-Lasso LV; Prosperi JR. Mechanisms of Taxane Resistance. *Cancers (Basel)*. **2020.** 12(11). doi: 10.3390/cancers12113323.
5. Alterio D; Marvaso G; Ferrari A; Volpe S; Orecchia R; Jereczek-Fossa BA. Modern radiotherapy for head and neck cancer. *Semin Oncol*. **2019**. 46(3): p. 233-245. doi: 10.1053/j.seminoncol.2019.07.002
6. De Ruysscher D; Niedermann G; Burnet NG; Siva S; Lee AWM; Hegi-Johnson F. Radiotherapy toxicity. *Nat Rev Dis Primers*. **2019.** 5(1): p. 13. doi: 10.1038/s41572-019-0064-5.

7. Gujral DM; Nutting CM. Patterns of failure, treatment outcomes and late toxicities of head and neck cancer in the current era of IMRT. *Oral Oncol*. **2018.** 86: p. 225-233. doi: 10.1016/j.oraloncology.2018.09.011.
8. Coppes RP; van der Goot A; Lombaert IM. Stem cell therapy to reduce radiation-induced normal tissue damage. *Semin Radiat Oncol*. **2009.** 19(2): p. 112-21. doi: 10.1016/j.semradonc.2008.11.005.
9. Kuhmann C; Weichenhan D; Rehli M; Plass C; Schmezer P; Popanda O. DNA methylation changes in cells regrowing after fractioned ionizing radiation. *Radiother Oncol*. **2011**. 101(1): p. 116-21. doi: 10.1016/j.radonc.2011.05.048.
10. Mothersill C; Seymour C. Are epigenetic mechanisms involved in radiation-induced bystander effects? *Front Genet*. **2012.** 3: p. 74. doi: 10.3389/fgene.2012.00074
11. Stone HB; Coleman CN; Anscher MS; McBride WH. Effects of radiation on normal tissue: consequences and mechanisms. *Lancet Oncol.* **2003**. 4(9): p. 529-36. doi: 10.1016/s1470-2045(03)01191-4.
12. Yarnold J; Brotons MC. Pathogenetic mechanisms in radiation fibrosis. *Radiother Oncol.* **2010.** 97(1): p. 149-61. doi: 10.1016/j.radonc.2010.09.002
13. Zhou Y; Sheng X; Deng F; Wang H; Shen L; Zeng Y; Ni Q; Zhan S; Zhou X. Radiation-induced muscle fibrosis rat model: establishment and valuation. *Radiat Oncol*. **2018.** 13(1): p. 160. doi: 10.1186/s13014-018-1104-0.
14. Baudelet M; Van den Steen L; Tomassen P; Bonte K; Deron P; Huvenne W; Rottey S; De Neve W; Sundahl N; Van Nuffelen G; Duprez F. Very late xerostomia, dysphagia, and neck fibrosis after head and neck radiotherapy. *Head Neck*. **2019.** 41(10): p. 3594-3603. doi: 10.1002/hed.25880.
15. Cox JD; Stetz J; Pajak TF. Toxicity criteria of the Radiation Therapy Oncology Group (RTOG) and the European Organization for Research and Treatment of Cancer (EORTC). *Int J Radiat Oncol Biol Phys*. **1995.** 31(5): p. 1341-6. doi: 10.1016/0360-3016(95)00060-C.
16. Offiah C; Hall E. Post-treatment imaging appearances in head and neck cancer patients. *Clin Radiol.* **2011.** 66(1): p. 13-24. doi: 10.1016/j.crad.2010.09.004.
17. Saito N; Nadgir RN; Nakahira M; Takahashi M; Uchino A; Kimura F; Truong MT; Sakai O. Posttreatment CT and MR imaging in head and neck cancer: what the radiologist needs to know. *Radiographics.* **2012.** 32(5): p. 1261-82; discussion 1282-4. doi: 10.1148/rg.325115160.
18. Wen X; Yu X; Cheng W; Li Y; Tian J. Quantitative Evaluation of Shear Wave Elastography on Radiation-Induced Neck Fibrosis in Patients With Nasopharyngeal Carcinoma. *Ultrasound Q.* **2019**. 37(2): p. 178-182. doi: 10.1097/RUQ.0000000000000452
19. Bardosi ZR; Dejaco D; Santer M; Kloppenburg M; Mangesius S; Widmann G; Ganswindt U; Rumpold G; Riechelmann H; Freysinger W. Benchmarking Eliminative Radiomic Feature Selection for Head and Neck Lymph Node Classification. *Cancers (Basel)*. **2022.** 14(3). doi: 10.3390/cancers14030477.
20. Gillies RJ; Kinahan PE; Hricak H. Radiomics: Images Are More than Pictures, They Are Data. *Radiology*. **2016.** 278(2): p. 563-77. doi: 10.1148/radiol.2015151169.
21. Ridner SH; Dietrich MS; Niermann K; Cmelak A; Mannion K; Murphy B. A Prospective Study of the Lymphedema and Fibrosis Continuum in Patients with Head and Neck Cancer. *Lymphat Res Biol.* **2016**. 14(4): p. 198-205. doi: 10.1089/lrb.2016.0001.
22. Steinbichler TB; Golm L; Dejaco D; Riedl D; Kofler B; Url C; Wolfram D; Riechelmann H. Surgical rescue for persistent head and neck cancer after first-line treatment. *Eur Arch Otorhinolaryngol*. **2020.** 277(5): p. 1437-1448. doi: 10.1007/s00405-020-05807-0
23. Steinbichler TB; Lichtenecker M; Anegg M; Dejaco D; Kofler B; Schartinger VH; Kasseroler MT; Forthuber B; Posch A; Riechelmann H. Persistent Head and Neck Cancer Following First-Line Treatment. *Cancers (Basel)*. 2018. 10(11). doi: 10.3390/cancers10110421
24. Boyd TS; Harari PM; Tannehill SP; Voytovich MC; Hartig GK; Ford CN; Foote RL; Campbell BH; Schultz CJ. Planned postradiotherapy neck dissection in patients with advanced head and neck cancer. *Head Neck.* **1998.** 20(2): p. 132-7. doi: 10.1002/(sici)1097-0347(199803)20:2<132::aid-hed6>3.0.co;2-3.
25. Denaro N; Russi EG; Numico G; Pazzaia T; Vitiello R; Merlano MC. The role of neck dissection after radical chemoradiation for locally advanced head and neck cancer: should we move back? *Oncology.* **2013.** 84(3): p. 174-85. doi: 10.1159/000346132.
26. Stenson KM; Haraf DJ; Pelzer H; Recant W; Kies MS; Weichselbaum RR; Vokes EE. The role of cervical lymphadenectomy after aggressive concomitant chemoradiotherapy: the feasibility of selective neck dissection. *Arch Otolaryngol Head Neck Surg*. **2000**. 126(8): p. 950-6. doi: 10.1001/archotol.126.8.950.
27. Lango MN; Andrews GA; Ahmad S; Feigenberg S; Tuluc M; Gaughan J; Ridge JA. Postradiotherapy neck dissection for head and neck squamous cell carcinoma: pattern of pathologic residual carcinoma and prognosis. *Head Neck*. **2009**. 31(3): p. 328-37. doi: 10.1002/hed.20976.
28. Moloney EC; Brunner M; Alexander AJ; Clark J. Quantifying fibrosis in head and neck cancer treatment: An overview. *Head Neck. 2015*. 37(8): p. 1225-31. doi: 10.1002/hed.23722.
29. Bourgier C; Auperin A; Rivera S; Boisselier P; Petit B; Lang P; Lassau N; Taourel P; Tetreau R; Azria D; Bourhis J; Deutsch E; Vozenin MC. Pravastatin Reverses Established Radiation-Induced Cutaneous and

Subcutaneous Fibrosis in Patients With Head and Neck Cancer: Results of the Biology-Driven Phase 2 Clinical Trial Pravacur. *Int J Radiat Oncol Biol Phys*. **2019.** 104(2): p. 365-373. doi: 10.1016/j.ijrobp.2019.02.024.

30. von Elm E; Altman DG; Egger M; Pocock SJ; Gøtzsche PC; Vandenbroucke JP. The Strengthening the Reporting of Observational Studies in Epidemiology (STROBE) statement: guidelines for reporting observational studies. *PLoS Med*. **2007.** 4(10): p. e296. doi: org/10.7892/boris.22114
31. Bossuyt PM; Reitsma JB; Bruns DE; Gatsonis CA; Glasziou PP; Irwig L; Lijmer JG; Moher D; Rennie D; de Vet HC; Kressel HY; Rifai N; Golub RM; Altman DG; Hooft L; Korevaar DA; Cohen JF. STARD 2015: an updated list of essential items for reporting diagnostic accuracy studies. *Bmj*. **2015.** 351: p. h5527. doi: 10.1136/bmj.h5527.
32. Swartz JE; Pothen AJ; Wegner I; Smid EJ; Swart KM; de Bree R; Leenen LP; Grolman W. Feasibility of using head and neck CT imaging to assess skeletal muscle mass in head and neck cancer patients. *Oral Oncol*. **2016.** 62: p. 28-33. doi: 10.1016/j.oraloncology.2016.09.006.
33. Zigon G; Berrino F; Gatta G; Sánchez MJ; van Dijk B; Van Eycken E; Francisci S. Prognoses for head and neck cancers in Europe diagnosed in 1995-1999: a population-based study. *Ann Oncol*. **2011**. 22(1): p. 165-174. doi: 10.1093/annonc/mdq306.
34. Dejaco D; Steinbichler T; Schartinger VH; Fischer N; Anegg M; Dudas J; Posch A; Widmann G; Riechelmann H. Prognostic value of tumor volume in patients with head and neck squamous cell carcinoma treated with primary surgery. *Head Neck.* **2018.** 40(4): p. 728-739. doi: 10.1002/hed.25040.
35. Dejaco D; Steinbichler T; Schartinger VH; Fischer N; Anegg M; Dudas J; Posch A; Widmann G; Riechelmann H. Specific growth rates calculated from CTs in patients with head and neck squamous cell carcinoma: a retrospective study performed in Austria. *BMJ Open*. **2019.** 9(2): p. e025359. doi: 10.1136/bmjopen-2018-025359
36. Dejaco D; Url C; Schartinger VH; Haug AK; Fischer N; Riedl D; Posch A; Riechelmann H; Widmann G. Approximation of head and neck cancer volumes in contrast enhanced CT. *Cancer Imaging*. **2015.** 15: p. 16. doi: 10.1186/s40644-015-0051-3.
37. Chamchod S; Fuller CD; Mohamed AS; Grossberg A; Messer JA; Heukelom J; Gunn GB; Kantor ME; Eichelberger H; Garden AS; Rosenthal DI. Quantitative body mass characterization before and after head and neck cancer radiotherapy: A challenge of height-weight formulae using computed tomography measurement. *Oral Oncol.* **2016**. 61: p. 62-9. doi: 10.1016/j.oraloncology.2016.08.012.
38. Choi Y; Ahn KJ; Jang J; Shin NY; Jung SL; Kim BS; Kim MS; Kim YS. Prognostic value of computed tomography-based volumetric body composition analysis in patients with head and neck cancer: Feasibility study. *Head Neck.* **2020**. 42(9): p. 2614-2625. doi: 10.1002/hed.26310.
39. Findlay M; White K; Stapleton N; Bauer J. Is sarcopenia a predictor of prognosis for patients undergoing radiotherapy for head and neck cancer? A meta-analysis. *Clin Nutr.* **2021.** 40(4): p. 1711-1718. doi: 10.1016/j.clnu.2020.09.017.
40. Grossberg AJ; Chamchod S; Fuller CD; Mohamed AS; Heukelom J; Eichelberger H; Kantor ME; Hutcheson KA; Gunn GB; Garden AS; Frank S; Phan J; Beadle B; Skinner HD; Morrison WH; Rosenthal DI. Association of Body Composition With Survival and Locoregional Control of Radiotherapy-Treated Head and Neck Squamous Cell Carcinoma. *JAMA Oncol*. **2016.** 2(6): p. 782-9. doi: 10.1001/jamaoncol.2015.6339.
41. Platek ME; Myrick E; McCloskey SA; Gupta V; Reid ME; Wilding GE; Cohan D; Arshad H; Rigual NR; Hicks WL Jr; Sullivan M; Warren GW; Singh AK. Pretreatment weight status and weight loss among head and neck cancer patients receiving definitive concurrent chemoradiation therapy: implications for nutrition integrated treatment pathways. *Support Care Cancer*. **2013.** 21(10): p. 2825-33. doi: 10.1007/s00520-013-1861-0.
42. Santer M; Kloppenburg M; Gottfried TM; Runge A; Schmutzhard J; Vorbach SM; Mangesius J; Riedl D; Mangesius S; Widmann G; Riechelmann H; Dejaco D; Freysinger W. Current Applications of Artificial Intelligence to Classify Cervical Lymph Nodes in Patients with Head and Neck Squamous Cell Carcinoma-A Systematic Review. *Cancers (Basel).* **2022.** 14(21). doi: 10.3390/cancers14215397.